Spectroscopic (UV, NMR) Investigation, Anti-Microbial And Molecular Docking Analysis Of 2,3-Dichloronaphthalene-1,4-Dione

Marshan Robert H, Amalanathan M, Usha D, Racil Jeya Geetha R, Sony Michael Mary M

Abstract : In the present study, the complete geometrical parameters of the 2,3-Dichloronaphthalene-1,4-dione (Dichlone) molecule were calculated with DFT method. UV-Vis spectra of the dichlone molecule have also been recorded and the electronic properties, viz. oscillator strengths, frontier orbital energies, excitation energies, calculated energies, and band gap energies are computed with TD-DFT method. The 1H and 13C NMR chemical shifts of the dichlone molecule have been calculated by the Gauge Independent Atomic Orbital (GIAO) method and compared with the experimental outcome. Docking studies were performed for dichlone molecule using the molecular docking software with four bacterial type (tubercular active) PDB's. In-vitro analysis had done with fungal and bacterial pathogens, Aspergillus niger and E.Coli.

Index terms : DFT; UV-Vis ; NMR ; Molecular Docking ; Anti-microbial

1. INTRODUCTION

Naphthoquinones are secondary metabolites of some fungi, plants, and bacteria, with antibiotic, antiviral, antifungal, antiparasitic, anti-inflammatory, antiproliferative, and cytotoxic activity. 2,3-Dichloronaphthalene-1,4-dione (Dichlone) is a fungicide and algicide of the quinone class. It is a general use fungicide applied to fruits, vegetables, field crops, ornamentals, and residential and commercial outdoor areas[1]. It is also used to control blue algae[2]. Dichlone is not persistent in soil and has moderate mammalian toxicity[2]. Dichlone can be manufactured by the chlorination and oxidation of naphthalene[3]. Recently, the antifungal and anti-bacterial activity of the nucleophilic substitution reactions of 1,4- naphthoquinone derivatives has been studied[4]. Moreover, the biological evaluation, antioxidant and cytotoxic activity of substituted 1,4-naphtho and benzoquinones have been investigated[5]. The title compound dichlone has many special properties and some unique characters because of the structure of quinone influence. In the present work, molecular geometry and optimized parameters of dichlone molecule are computed and the performance of the computational method for B3LYP with the standard 6-311++G(d,p) basis set. Absorption maximum peak of dichlone molecule is obtained from the UV-visible spectrum. In order to provide information on the transfer of charges within the compound, several properties such as HOMO, LUMO, total partial and overlap population density-of-states are carried out. Chemical shifts from the NMR spectrum are predicted. Dichlone molecule anti-tuberculosis activity was analyzed by molecular docking studies. Dichlone molecule hydrogen bonding interaction with various PDB is used to predict the compound's excellent binding area. In addition to the above, this study provides comprehensive information on the anti-microbial activity of the dichlone molecule.

2. COMPUTATIONAL DETAILS

The entire theoretical calculations were performed DFT method at B3LYP/6-311++G(d,p) basis set to using Gaussian 09W programs [6]. The electronic properties such as HOMO and LUMO energies were determined by time dependent TD-DFT approach [7]. 1H and 13C NMR isotropic shielding were calculated by GIAO method [8] using optimized parameters obtained from B3LYPwith 6-311++G (d,p) method. AutoDock4 (version 4.2) with the Lamarckian genetic algorithm was used to perform docking studies[9].

3. EXPERIMENTAL DETAILS

The dichlone molecule in the solid form was purchased from sigma Aldrich chemical company (USA) with a stated purity of greater than 98% and it was used as such without further purification. Acetone is used as a solvent (Perkin Elmer LAMBDA 950), the UV-Visible spectrum of the compound was recorded in the range of 200-800 nm using UV-Visible Spectrophotometer. The 1H and 13C NMR spectra are taken in acetone solutions and all signals are referenced to TMS on a BRUKER AVANCE III500 MHz (AV500) Spectrometer. All NMR spectra are recorded at room temperature. The spectral measurements were carried out at Regional Sophisticated Instrumentation Centre, IIT, Chennai, Tamil Nadu, India.

- *Marshan Robert H - Research scholar, Reg. No: 17233282131011, Manonmaniam Sundaranar University, Abishekapatti, Tirunelveli 627 012, Tamilnadu, India.*
- *Department of Physics & Research centre, Women's Christian College, Nagercoil, Tamilnadu, India.*
- *Amalanathan M -Department of Physics & Research Centre, Nanjil Catholic College of Arts and ScienceKaliyakkavilai,Tamil Nadu, India*
- *Usha D - Department of Physics & Research centre, Women's Christian College, Nagercoil, Tamilnadu, India*
- *Racil Jeya Geetha R - Department of Physics &Research Centre, Nesamony Memorial Christian College, Marthandam - Tamil Nadu, India.*
- *Sony Michael Mary M - Research Scholar, Register Number: 19113112132006, ManonmaniamSundaranar University, Abishekapatti, Tirunelveli, Tamil Nadu, India.*

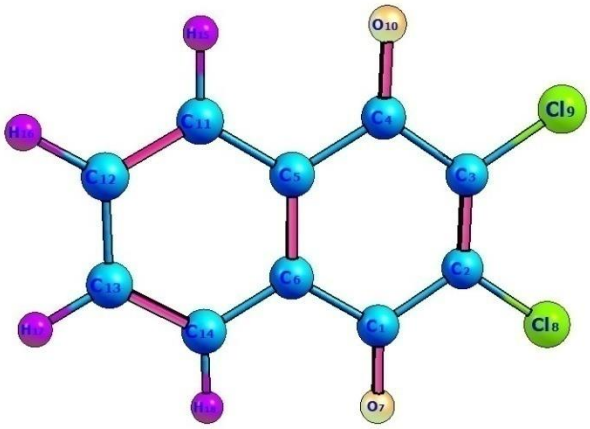

Figure 1: Optimized geometry of Dichlone moecue

4. RESULTS AND DISCUSSION

4.1 Optimized geometry

Dichlone molecule structure was optimized using the B3LYP method with a 6-311++G (d,p) basis set. The optimized molecular structure of the dichlone molecule is shown in Figure 1. The optimized geometrical parameter of the dichlone molecule is given in Table 1. The calculated values were compared with the X-ray diffraction results [10], [11]. From the computational values, the calculated parameters are slightly increased or decreased from observed values, due to fact that the computational works belong to molecule in the gaseous phase and the observed results belong to molecule in solid state. The molecule has nine C-C bond lengths, four C-H bond lengths, two C-O and two C-Cl bond length. The chlorine and oxygen atoms are substituted in the place of hydrogen atoms, which make the dichlone molecule fused ring angles appear as slightly out of planar structure. The C-C bond length value of the ring is varied between 1.3515 - 1.502 Å. The substituted chlorine atoms make the larger bond length with the neighbouring C1-C2 (1.502 Å) and C3-C4 (1.502 Å) atoms. From the computational results, the value of C-Cl (1.7246 Å) bond length is found to be high compared to other bond length values. The bond angles C1–C2–C3 and C2–C3–C4 are increased by 1.8981^{o} from the normal bond angle value 120^{o}, which makes the asymmetry nature of the exocyclic angles at the C2 and C3 positions reveals the repulsion between chlorine atoms and the fused ring system. The other important bond length and bond angle values are presented in table 1.

TABLE 1

Optimized geometric parameters

Bond length	Values(Å)		Bond angle	Values(º)	
	Cal.	Exp.		Cal.	Exp.
C_1-C_2	1.502	1.491	C_1-C_2-C_3	121.89	122.14
C_2-C_3	1.351	1.337	C_2-C_3-C_4	121.89	122.54
C_3-C_4	1.502	1.493	C_3-C_4-C_5	117.03	116.72
C_4-C_5	1.488	1.480	C_4-C_5-C_6	121.06	120.79
C_5-C_6	1.402	1.395	C_6-C_1-O_7	122.19	121.22
C_1-O_7	1.213	1.219	C_1-C_2-Cl_8	115.42	116.03
C_2-Cl_8	1.724	1.707	C_2-C_3-Cl_9	122.67	121.59
C_3-Cl_9	1.724	1.711	C_3-C_4-O_{10}	120.77	121.79
C_4-O_{10}	1.213	1.216	C_4-C_5-C_{11}	119.03	119.18
C_5-C_{11}	1.396	1.390	C_5-C_{11}-C_{12}	119.91	119.74
C_{11}-C_{12}	1.391	1.386	C_{11}-C_{12}-C_{13}	120.18	120.52
C_{12}-C_{13}	1.396	1.383	C_{12}-C_{13}-C_{14}	120.18	120.12
C_{13}-C_{14}	1.391	1.386	C_{12}-C_{11}-H_{15}	121.35	120.15
C_{11}-H_{15}	1.082	0.950	C_{13}-C_{12}-H_{16}	120.01	119.71
C_{12}-H_{16}	1.083	0.950	C_{14}-C_{13}-H_{17}	119.80	119.95
C_{13}-H_{17}	1.083	0.950	C_6-C_{14}-H_{18}	118.72	120.05
C_{14}-H_{18}	1.082	0.950			

4.2 UV-Visible spectral analysis

The electronic spectrum of the dichlone compound was recorded from 200 nm to 800 nm. Experimental UV-vis spectra are shown in Figure 2; acetone is used as solvent for both theoretical and experimental analysis. The computational UV-visible absorption spectra were calculated using the TD–DFT method based on the B3LYP/6–311++G(d,p) level of theory. The observed and computed wavelength (λ), the corresponding electronic excitation energies, oscillator strength (f) and the transition nature are listed in Table 2. The electronic spectrum shows five absorption bands at 414, 373, 337, 258 and 230 nm due to π → π* and n → π* transitions respectively[12]. The theoretical absorption bands are at 416.44, 407.41 and 386.66 nm in solvent phase. It is found that the higher computed λ values of the dichlone molecule are in agreement with the experimental value. The absorption band with higher intensity (λ_{max}= 414 nm) corresponds to HOMO-2 → LUMO transition and dichlone molecule higher intensity transistion is mainly characterized as n → π* type transition with higher oscillator strength 0.0054 [13]. The calculated value for higher intensity band is λmax= 416.44 nm(calculated). This higher intensity wavelength shows the presence of more number of free lone pairs of electrons from electronegative chlorine and oxygen atoms of the dichlone molecule. The electronic transition from the HOMO-2 → LUMO with 98% contribution is corresponds to maximum absorption wavelength is assigned for band gap energy 2.996 eV and the corresponding calculated band gap energy is 2.979 eV. The wavelength with moderate oscillator strength 0.0033 is assigned to the transition from the HOMO to LUMO with 98 percent contributions. The third maximum absorption wavelength is assigned for transition on HOMO-4 → LUMO with 97% contribution. The HOMO to LUMO 98 percent maximum contribution with band gap energy 3.325eV shows the transfer of electron from the ring to the electronegative atoms oxygen and chlorine. Lowering of the HOMO - LUMO energy gap 3.325eV explains eventual charge transfer interactions taking place within the molecule and the biological activity of the title compound dichlone.

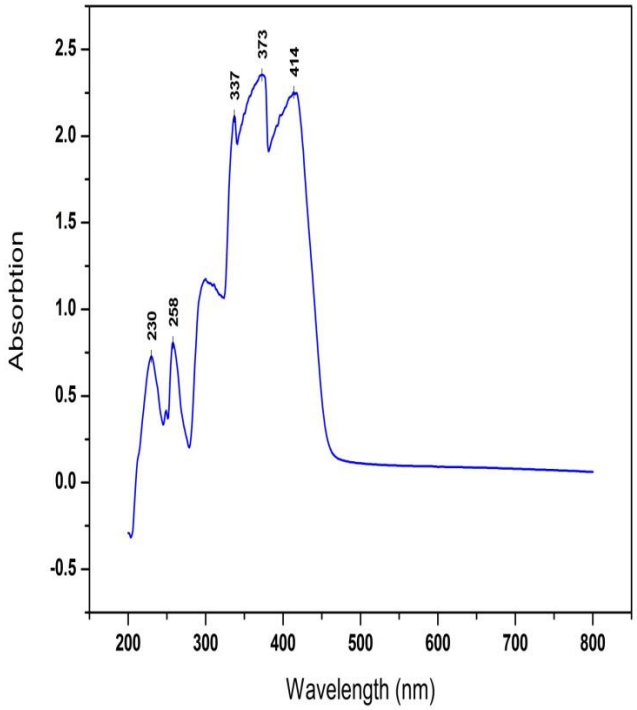

4.3 Total partial and overlap population density-of-states.

The total (TDOS), partial (PDOS) and overlap population (OPDOS or COOP (Crystal Orbital Overlap Population)) density of sates was created to convoluting the molecular orbital information using the Gaussum2.2 Program [14]. The TDOS, PDOS and OPDOS spectrum of dichlone molecule is plotted in figure 3a-3c.

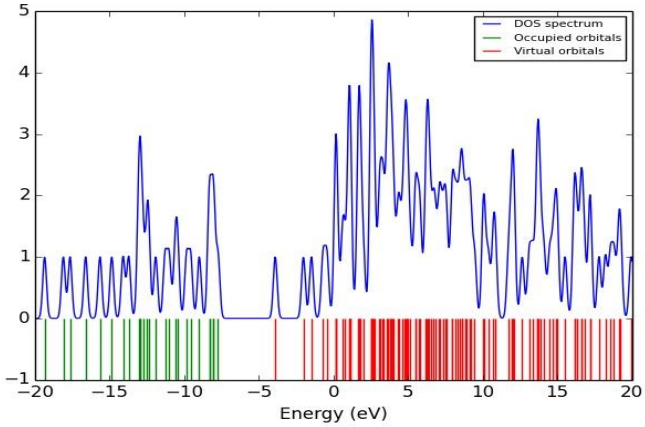

Figure 3a: DOS spectrum of Dichlone molecule

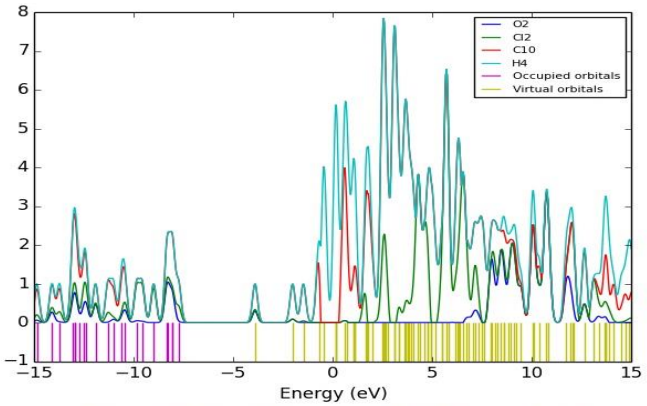

Figure 3b: PDOS Spectrum of Dichlone molecule

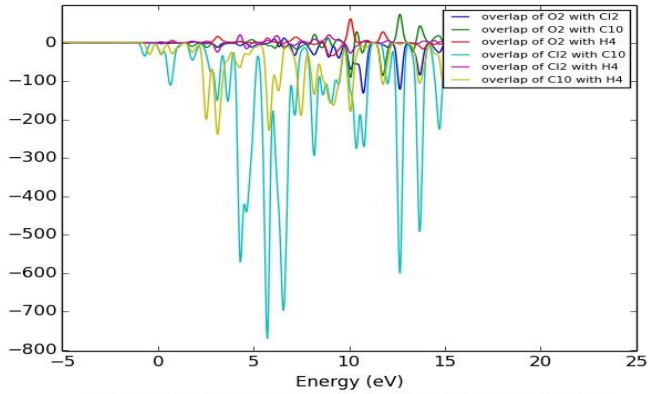

Figure 3c: COOP Spectrum of Dichlone molecule

They provide a pictorial representation of MO composition and their contributions to the chemical bonding . The OPDOS show the bonding, anti-bonding and nonbonding nature of the interaction of the two orbitals. The positive value of OPDOS indicates a bonding interaction; negative value means that there is an anti-bonding interaction and zero value shows non-bonding interaction [15]. From the dichlone molecule PDOS spectrum, the C atom having 60% contribution in HOMO and C atom having 66% contribution in LUMO were predicted the bonding interactions with positive values which reveals the MOs mainly localized on ring and electronegative atoms of the dichlone molecule. From the COOP spectrum, overlap of C with Cl and C with H atoms of dichlone molecule show the maximum negative peak, this exhibits strong anti-bonding interaction with overlap population value. It confirms the biological activity of the title molecule dichlone.

TABLE 2: UV-visible datas

4.4 Natural charge analysis

The natural population analysis [16] performed for the title molecules clearly depict the distribution of charges in the various sub shells in the molecular orbital. The accumulation of natural charges on an individual atom of the title molecules is given in Table 3.

TABLE 3: *Natural charges of Dichone molecule*

Atoms	Natural charges
C_1	0.51311
C_2	-0.11462
C_3	-0.11127
C_4	0.50075
C_5	-0.11048
C_6	-0.11731
O_7	-0.50464
Cl_8	0.0954
Cl_9	0.09557
O_{10}	-0.50387
C_{11}	-0.14734
C_{12}	-0.17339
C_{13}	-0.17351
C_{14}	-0.14724
H_{15}	0.23528
H_{16}	0.21421
H_{17}	0.21421
H_{18}	0.23532

The natural charge chart of dichlone molecule is presented in figure 4. The natural atomic charge of C1 and C4 atom are bonded with more electro-negative oxygen atoms (O) due to the intramolecular interaction these atoms have more positive charges compared with other carbon atoms. An oxygen atom O7 has the most electronegative charge and carbon atom C1 has the most electropositive charge. Likewise, C2, C3, C5, C6, C11, C12, C13 and C14 atoms have considerable electronegativity and they tend to donate an electron. Conversely, the Cl8, Cl9, H15, H16, H17 and H18 atoms have considerable electropositive and they tend to acquire an electron.

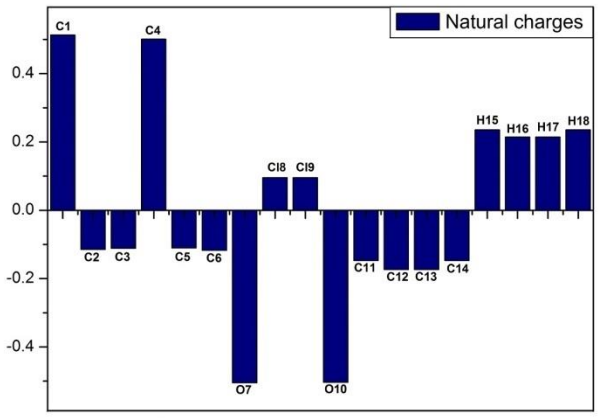

Figure 4: Natural charges of Dichlone molecule

4.5 NMR Analysis

The gauge invariant atomic orbital (GIAO) 1H and 13C calculations of dichlone molecule are calculated and compared with experimental data which are presented in Table 4. The observed 13C and 1H NMR spectra of the title compound in acetone solvent are shown in Figure 5a & 5b. The B3LYP / GIAO model calculated the absolute isotropic chemical shielding of dichlone molecule [17]. Relative chemical shifts were then estimated using the corresponding TMS shielding : σcalc (TMS) is calculated in advance at the same theoretical level. Numerical values of chemical shift δpred = σ calc(TMS) - σ calc together with calculated values of σ calc(TMS), are given in Table 4.

Experimental		Theoretical				Assignments
(λ_{max})nm	Band Gap(eV)	(λ_{max}) nm	Band Gap(eV)	Energy (cm^{-1})	Oscillator Strength(f)	Major contribution
414	2.996	416.4	2.979	24012	0.0054	H-2→LUMO (98%)
373	3.3625	407.4	3.045	24545	0.0033	HOMO→LUMO (98%)
337	3.681	386.6	3.208	25862	0.0054	H-4→LUMO (97%)

TABLE 4*: ^{13}C and ^{1}H NMR*

ATOMS	THEORITICAL	EXPERIMENTAL
C_1	183.0485	175.959
C_2	158.146	143.011
C_3	158.146	143.011
C_4	183.0485	175.959
C_5	135.1174	131.263
C_6	135.1174	131.263
C_{11}	132.4125	127.238
C_{12}	140.7932	134.662
C_{13}	140.7932	134.662
C_{14}	132.4125	127.238
H_{15}	8.85	8.193
H_{16}	8.52	7.973
H_{17}	8.52	7.973
H_{18}	8.85	8.193

The range of 13C NMR shifts for aromatic carbon atoms normally exceeds 100 ppm[18]. The chemical shifts of the whole dichlone molecule 13C NMR signals are greater than 100 ppm as expected in the literature. The predicted shifts in carbon atoms are in the range of 132.4125-183.0485 for the title compound, and these values correspond to the experimental range of chemical shifts 127.238-175.959 ppm. The atom C1 's and C4 's chemical shifts observed at 175.959 ppm are due to the electronegative nature of oxygen atoms and the partial ionic nature of the group C= O.

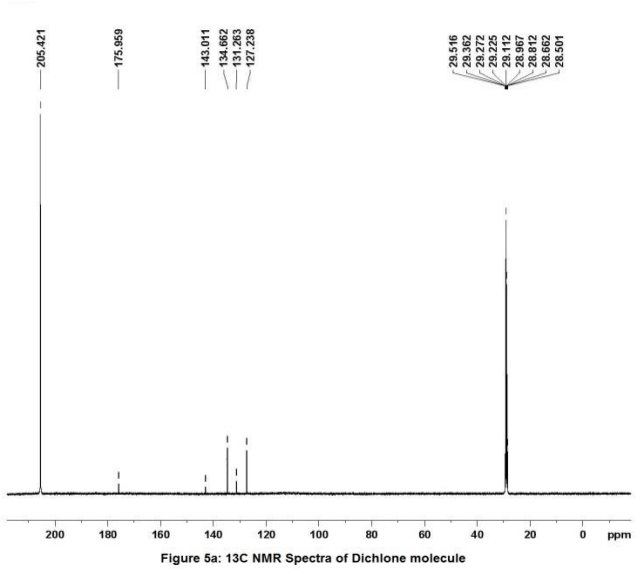

Figure 5a: 13C NMR Spectra of Dichlone molecule

The C1 's and C4 's carbon atom's predicted chemical shifts are 183.0485 ppm. The oxygenated (C1 & C4) and chlo-rinated (C2 & C3) chemical shift value of carbon atoms are high, compared to other aromatic carbon atoms. The experimental proton NMR spectrum of dichlone molecule is shown in Figure 5b and the result shows that there are two types of similar protons.

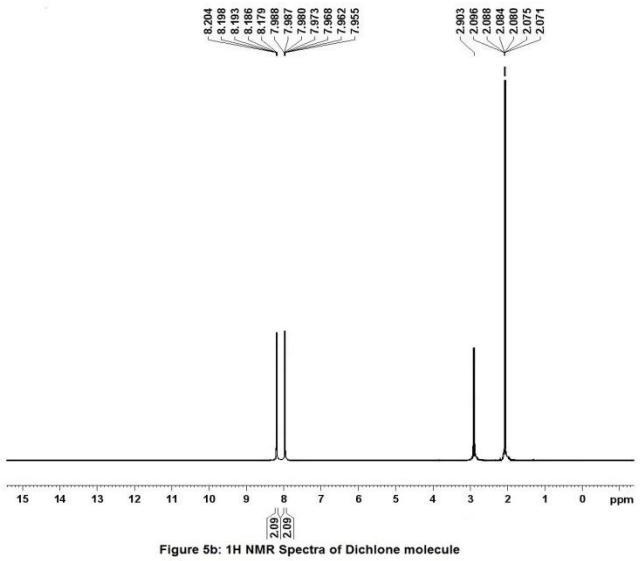

Figure 5b: 1H NMR Spectra of Dichlone molecule

The doublet at δ 8.193 has been attributed at H15 and H18 of dichlone molecule ring and H15 and H18 atom shows an increase in chemical shift (8.193 ppm) due to the oxygen atom's influence. The doublet at δ 7.973 has been attributed at H16 and H17 of dichlone molecule ring. The predicted chemical shifts of dichlone molecule are in accordance with the experimental values and the results are presented in table 4.

4.6. Fukui Functions

The Fukui indices are, in short, reactivity indices they give us info concerning that atoms during a molecule have a large tendency to either loose or accept an electron, which we tend to chemist interpret as that are a lot of susceptible to endure a nucleophilic or an electrophilic attack, respectively. The Fukui function is defined as [19].

$$F=((\delta\rho(r))/\delta N)r$$

Where ρ(r) is the electron density, N is the number of electrons, r is that the external potential. The Fukui function is a local reactivity descriptor which gives the preferred regions where a chemical species will change its density when the number of electrons is modified. Hence, Fukui function indicates the propensity of the electronic density to deform at a given position upon accepting or donating electrons [20], [21] and the corresponding condensed or atomic Fukui functions on the jth atom site are given as,

$$Fj+ = Qj\ (N+1) - Qj\ (N)$$
$$Fj- = Qj\ (N) - Qj\ (N-1)$$
$$Fj0 = 1/2\ [\ Qj\ (N+1) - Qj\ (N-1)]$$

The electrophilic, nucleophilic and free radical on the reference molecule denoted by the symbol Fj-, Fj+, Fj0 respectively. In the above equations, Qj is that the atomic charge at the jth atomic site is the neutral (N), anionic (N+1) or (N-1) chemical species. Chattaraj et al. [22] have introduced the thought of generalized philicity. It contains the majority info concerning hitherto well-known completely different global and local reactivity and selectivity descriptor, in additionally to the data concerning electrophilic/nucleophilic power of a given atomic site during a molecule. Morell et al. [23] have recently planned a dual descriptor ΔF(r), which is defined as the difference between the nucleophilic and electrophilic Fukui function and is given by the equation,

$$\Delta F(r) = [F+(r) - F-(r)]$$

The site is favored for a nucleophilic attack whereas dual descriptor ΔF(r)>0 and the site is favored for an electrophilic attack whereas dual descriptor ΔF(r)<0. According to dual descriptor ΔF(r) give a transparent distinction between nucleophilic and electrophilic attack at a particular site with their sign. That is they provide positive value prone for electrophilic attack. Dual descriptor values are reported in Table 5, according to the condition for dual descriptor, nucleophilic site for in our dichlone molecule is C2, C3, C5, C6, O7, O10, C11, C12, C13 and C14 are Positive values i.e. ΔF (r)>0. Similarly the electrophilic site is C1, C4, Cl8, Cl9, H15, H16, H17 and H18 Negative values i.e. ΔF(r)<0. The behavior of molecule as electrophilic and nucleophilic attack throughout reaction depends on the local behavior of molecule.

TABLE 5: *Fukui functions (f_j+, f_j-, f_j0)*

f_j+	f_j-	f_j0	f(r)
-0.43991	0.057277	-0.19132	-0.49719
0.304489	0.03059	0.16754	0.273899
0.304489	0.03059	0.16754	0.273899
-0.43991	0.057277	-0.19132	-0.49719
0.115976	0.010388	0.063182	0.105588
0.115976	0.010388	0.063182	0.105588
0.41999	0.109613	0.264802	0.310377
0.073581	0.136343	0.104962	-0.06276
0.073581	0.136342	0.104962	-0.06276
0.419985	0.109615	0.2648	0.31037
0.04163	0.01747	0.02955	0.02416
0.230256	0.018	0.124128	0.212256
0.230255	0.018001	0.124128	0.212254
0.04163	0.01747	0.02955	0.02416
-0.13021	0.051362	-0.03942	-0.18157
-0.1158	0.06895	-0.02342	-0.18475
-0.1035	0.06895	-0.01727	-0.17245
-0.13021	0.051362	-0.03942	-0.18157

4.7 Anti- microbial Assay

The method of diffusion of the agar well is widely used to assess the compound's antimicrobial activity. Mueller-Hinton agar autoclaved 15-20 ml was poured on glass petri plates and solidified. The test organism's standardized inoculum was uniformly spread using sterile cotton swab on the surface of these plates. With a sterile cork borer in each plate, four wells with a diameter of 8 mm (20 mm apart from each other) were punched aseptically. The sample (40 and 80µL) was added to two of the wells at the desired concentration of 100 mg / mL and one well with Gentamycin as a positive and compound solvent as a negative control for bacterial and Clotrimazole as positive and compound solvent as negative control for fungai . The agar plates were then incubated for 24 hours under 37 °C. Clear zone was observed after incubation. Bacterial and fungai growth inhibition was measured in mm.

Figure 6: Anti-microbial activity of Dichlone molecule

Observation :The anti-bacterial activity of dichlone molecule, was tested against bacterial strain E. coli indicate that bacterial species exhibit different sensitivities and the required results has been compared with the inhibition diameter of positive control i,e. Gentamycin drug, with variable extent. The diameter of inhibition zone of the dichlone molecule were 18 mm at 40µL and 22 mm at 80µL, for the strains E.coli and that diameter of inhibition zone revealed anti-bacterial activity however, which is less than standard Table 6. The anti-fungai activity of dichlone molecule, was tested against fungai strain aspergillus niger indicate that fungai species exhibit different sensitivities and the required results has been compared with the inhibition diameter of positive control i,e. Clotrimazole drug, with variable extent. The diameter of inhibition zone of the dichlone molecule were 10 mm at 40µL and 22 mm at 15µL, for the strains aspergillus niger and that diameter of inhibition zone revealed anti-fungai activity however, which is less than standard Table 6. The antibacterial and anti-fungai activity of the dichlone molecule at different concentrations for antibacterial pathogens E.coli and anti-fungai pathogens aspergillus niger are shown in Figure 6.

***TABLE 6**: Anti-microbial activity of Dichlone molecule*

Sample	E.coli				A.niger			
	+	-	T1	T2	+	-	T1	T2
Nicotinic Hydrazide	32	-	18	22	20	-	10	15

4.8 Molecular Docking

The structure of title compound was optimized based on the density functional theory using Gaussian 09 program. The molecular docking was performed using AutoDock Tools-1.5.4 interfaced with the MGL Tools-1.5.4 package [24].

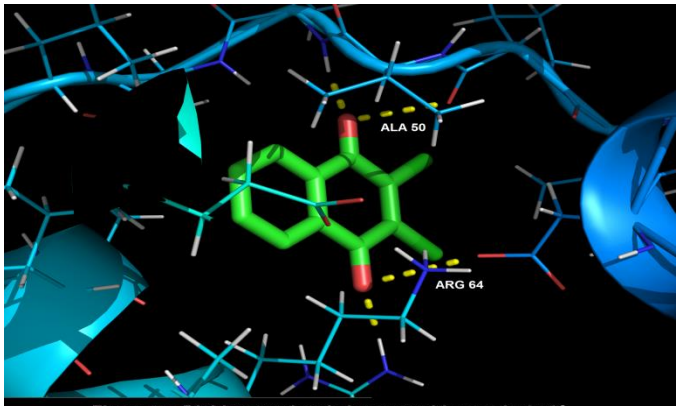

Figure 7a: Dichlone molecule interact with protein 1w6f

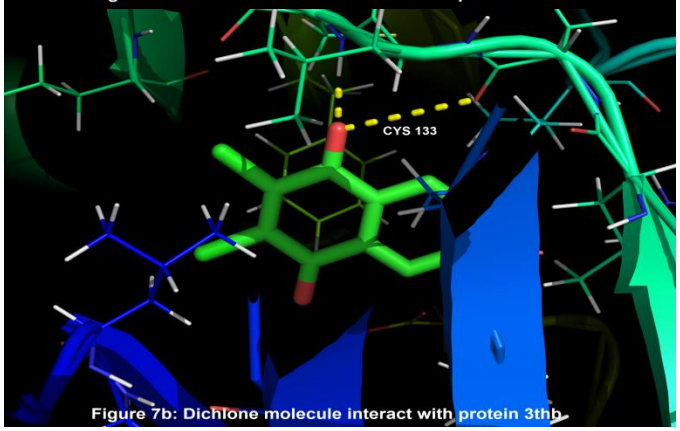

Figure 7b: Dichlone molecule interact with protein 3thb

The Mycobacterium tuberculosis enoyl reductase (INHA) type proteins (PDB ID: 1W6F, 3THB, 4B55, 4C5P) was selected for the present docking analysis. The three-dimensional (3D) coordinates of the protein file was downloaded from the Research Collaboratory for Structural Bioinformatics (RCSB) protein data bank [25]. The protein preparation has been carried out by the following steps (i) all water molecules were removed (ii) hydrogen atoms were added to the crystal structure (iii) add Coulomb charges (iv) and previous docked inhibitor was removed from all the proteins.

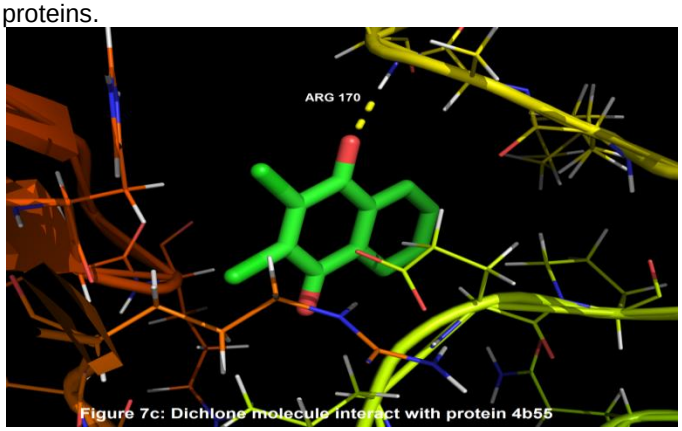

Figure 7c: Dichlone molecule interact with protein 4b55

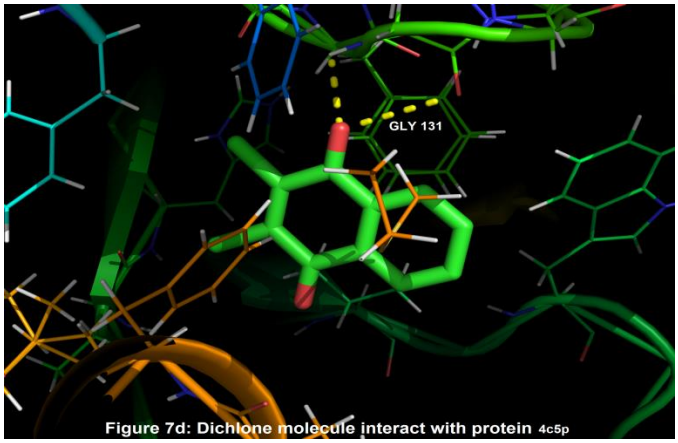

Figure 7d: Dichlone molecule interact with protein 4c5p

TABLE 7: *Dichlone molecule interact with different proteins*

Protein (PDB:ID)	Binding Residue	Bond distance (Å)	Incubation constant (µm)	Binding affinity (k/cal)
1W6F	ALA 50	1.95	39.92	-6.0
	ARG 64	1.86		
3THB	CYS 133	1.71	19.85	-6.42
4B55	ARG 170	1.86	21.17	-6.38
4C5P	GLY 131	2.30	1.03	-8.17

The AutoGrid 4.2 [26], [27] was used to create affinity grids centered on the active site with maximum grid size. The rigid protein and flexible ligand dockings were performed by using AutoDock 4.2 with the Lamarckian genetic algorithm. The docking results were evaluated by sorting the binding free energy predicted by docking confirmations. All the selected proteins are docked with the title molecule dichlone and the best confirmation binding energy was observed in one of the selected target protein 4C5P with ligand was -8.17 kcal/mol. The amino acid GLY 131 present in the active site of the target protein binds with the ligand by N–H…..O hydrogen bonding. The most conformation binding energy of selected target proteins with ligands are listed in Table 7. The protein-ligand interaction of selected proteins and title compound is shown in figures 7a-7d. The most conformation binding energy -8.17kcal/mol reveals the title molecule dichlone has anti-tubercular activity.

5. CONCLUSION

The optimized geometry of the title compound dichlone were determined using the basic set of DFT / B3LYP / 6-311 ++ G (d, p). The electronic spectrum of the dichlone compound shows lowering of the HOMO - LUMO energy gap 3.325eV explains eventual charge transfer interactions taking place within the molecule and the biological activity of the title compound dichlone. In NMR spectral analysis, the H15 and H18 atom shows an increase in chemical shift (8.193 ppm) due to the oxygen atom's influence. The shielding effect of the atom C1 's and C4 's chemical shifts observed at 175.959 ppm are due to the electronegative nature of oxygen atoms and the partial ionic nature of the group C= O. The activity of dichlone molecule against the PDB (4C5P) is significant with a binding energy of -8.17kcal / mol, which indicates that dichlone may exhibit significant anti-tubercular activity against the variety tubercular breed by targeting the PDB (4C5P). In vitro anti-microbial studies suggest that the title compound is less anti-bacterial against E.coli and less anti-fungui against aspergillus niger. It can therefore be concluded from the above research that title compound dichlone has biological activity included anti-tuberculor activity.

REFERENCE

[1] "Dichlone (Phygon, Quintar) Chemical Profile". Pesticide Management Education Program, Cornell Cooperative Extension.

[2] "Dichlone". Pesticide Properties DataBase, University of Hertfordshire.

[3] A.Thomas Unger, Pesticide Synthesis Handbook. 1996, 966. ISBN 0-8155-1853-6.

[4] C. Ibis, A.F. Tuyun, H. Bahar, S.S. Ayla, M.V. Stasevych, R.Y. Musyanovych, O.K. Porokhnyavets and V. Novikov, Medicinal Chemistry Research, 2014, 23, 2140, DOI:10.1007/s00044-013-0806-y

[5] N.G. Deniz, C. Ibis, Z. Gokmen, M. Stasevych, V. Novikov, O.K. Porokhnyavets, M. Ozyurek, K. Guclu, D. Karakas and E. Ulukaya, Chemical and Pharmaceutical Bulletin,2015, 63, 1029, DOI:10.1248/cpb.c15-00607

[6] M.J. Frisch, G.W. Trucks, H.B. Schlegel, G.E. Scuseria, M.A. Robb, J.R. Cheeseman, G. Scalmani, V. Barone, B. Mennucci, G.A. Petersson, H. Nakatsuji, M. Caricato, X. Li, H.P. Hratchian, A.F. Izmaylov, J. Bloino, G. Zheng, J.L. Sonnenberg, M. Hada, M. Ehara, K. Toyota, R. Fukuda, J. Hasegawa, M. Ishida, T. Nakajima, Y. Honda, O. Kitao, H. Nakai, T. Vreven, J.A. Montgomery Jr., J.E. Peralta, F. Ogliaro, M. Bearpark, J.J. Heyd, E. Brothers, K.N. Kudin, V.N. Staroverov, R. Kobayashi, J. Normand, K. Raghavachari, A. Rendell, J.C. Burant, S.S. Iyengar, J. Tomasi, M. Cossi, N. Rega, J.M. Millam, M. Klene, J.E. Knox, J.B. Cross, V. Bakken, C. Adamo, J. Jaramillo, R. Gomperts, R.E. Stratmann, O. Yazyev, A.J. Austin, R. Cammi, C. Pomelli, J.W. Ochterski, R.L. Martin, K. Morokuma, V.G. Zakrzewski, G.A. Voth, P. Salvador, J.J. Dannenberg, S. Dapprich, A.D. Daniels, O. Farkas, J.B. Foresman, J.V. Ortiz, J. Cioslowski, D.J. Fox, Gaussian 09, Revision A.02, Gaussian, Inc., Wallingford CT, 2009.

[7] D. Arul Dhas, I. Hubert Joe, S.D.D. Roy, S. Balachandran, DFT computation and experimental analysis of vibrational and electronic spectra of phenoxy acetic acid herbicides, Spectrochim. Acta, Part A 2013, 108, 89-99. https://www.researchgate.net/publication/235880479.

[8] N.M.O. Boyle, A.L. Tenderholt, K.M. Langner, Software news and updates cclib: a library for package-independent computational chemistry algorithms, J. Comput. Chem. 2008, 29(5), 839-

845.
https://www.ncbi.nlm.nih.gov/pubmed/17849392.
[9] G.M. Morris, R. Huey, W. Lindstrong, M.F. Sanner, R.K. Belew, D.S. Goodsell, A.J. Olson, Software news and updates AutoDock4 and AutoDockTools4: automated docking with selective receptor flexibility, J. Comput. Chem. 2009, 16, 2785-2791.
[10] M.Ukaegbu, R.J.Butcher, N.M.Enwerem, O.Bakare and C.Hosten '2,3-Di-chloro-5,8-dimeth--oxy-1,4-naphtho-quinone'Acta Cryst. 2012, E68, o2018 https://doi.org/10.1107/S1600536812023926
[11] D. E. Lynch and I. McClenaghan '2-Chloro-3-(4-methyl¬piperazino)-1,4-naphtho¬quinone'Acta Cryst. 2001, E57, o287-o288 https://doi.org/10.1107/S1600536801003634
[12] S.R. Layana, S.R. Saritha, L. Anitha, M. Sithambaresan, M.R. Sudarsanakumar, S.Suma, J. Mol. Struct. 2018, 1157, 579–586.
[13] V. Hriday Narayan Mishra, Onkar Prasad, Leena Sinha, Computational and Theoretical Chemistry, 2011, 973, 20–27.
[14] N.M. O' Boyle, A.L. Tenderholt, K.M. Langer, cclib: A library for package-independent computational chemistry algorithms, J. Comput. Chem. 2008, 29, 839–845. https://doi.org/10.1002/jcc.20823
[15] M. Chen, U.V. Waghmare, C.M. Friend, E. Kaxiras, A density functional study of clean and hydrogen-covered α-MoO3(010):Electronic structure and surface relaxation, Journal of Chemical Physics, 1998, 109, 6854-6860.
[16] A. E. Reed, R. B. Weinstock, and F.Weinhold, "Natural populationanalysis," The Journal of Chemical Physics, 1985, 83(2), 735–746.
[17] K.Wolinski, J.F.Hinton, P.Pulay, Efficient implementation of the gauge-independent atomic orbital method for NMR chemical shift calculations , J. Am. Chem. Soc. 1990, 112, 8251–8260. https://pubs.acs.org/doi/10.1021/ja00179a005
[18]] S. Ahmad, S. Mathew, P.K. Verma, Laser Raman and FT-infrared spectra of 3,5-dinitrobenzoic acid, Indian J. Pure Appl. Phys. 1992, 30, 764-765.
[19] P.W.Ayers, R.G. Parr, Variational Principles for Describing Chemical Reactions: The Fukui Function and Chemical Hardness Revisited, J. Am. Chem. Soc.2000, 122 , 2010-2018.
[20] R.G.Parr, amd W. Uang, Density functional approach to the frontier-electron theory of chemical reactivity, J. Am. Chem. Soc. 1984, 106, 4049-4050.
[21] P.K.Chattaraj, B. Maiti, U. Sarkar, Philicity, A Unified Treatment of Chemical Reactivity and Selectivity, J. Phys. Chem. A, 2003, 107, 4973–4975.
[22] C.Morell, A.Grand, A.Toro-Labbe, New Dual Descriptor for Chemical Reactivity, J. Phys. Chem. A, 2005, 109, 205–212.
[23] E.Scroco, J. Tomasi, Adv, Electronic Molecular Structure, Reactivity and Intermolecular Forces: An Euristic Interpretation by Means of Electrostatic Molecular Potentials, Quantum chem. 1979, 11, 115-193.
[24] G.M.Morris, R.Huey, W.Lindstrom, M.F.Sanner, R.K.Belew, D.S.Goodsell, A.J.Olson, AutoDock4 and AutoDockTools4: Automated docking with selective receptor flexibility. J. Comput. Chem. 2009, 16, 2785–2791.
[25] F.C.Bernstein, T.F.Koetzle, G.J.Williams, E.E. Meyer, M.D.Brice, J.R.Rodgers, O.Kennard, T.Shimanouchi, M.Tasumi, The Protein Data Bank: A computer-based archival file for macromolecular structures. J. Mol. Biol. 1977, 112, 535–542.
[26] G.M.Morris, D.S.Goodsell, R.S.Halliday, R.Huey, W.E.Hart, R.K.Belew, A.J.Olson, Automated docking using a Lamarckian genetic algorithm and an empirical binding free energy function. J. Comput. Chem. 1998, 19, 1639–1662.
[27] R.Huey, G.M.Morris, A.J.Olson, D.S.Goodsell, A semiempirical free energy force field with charge-based desolvation. J. Comput. Chem. 2007, 28, 1145–1152.